ISSN 2682-681X (Paper), ISSN 2705-4241 (Online) | http://unilorinjoger.com | https://doi.org/10.63745/jogersi.2026.06.30.009

JOGER SPECIAL ISSUE, 2026

JOURNAL OF GEOMATICS AND ENVIRONMENTAL RESEARCH http://www.unilorinjoger.com

Geospatial Analysis of Land Use and Land Cover Changes Over Daura, Katsina State

Olusesi Oluseyi Christiana, Usman Shehu Shitu & Ngurnoma Yerima Nuhu

Department of Geomatics, Ahmadu Bello University, Zaria, Nigeria

*Corresponding author email: christianaolusesi20@gmail.com

Abstract

Land use and land cover (LULC) change in semi-arid northern Nigeria is driven by settlement expansion, agricultural pressure and climatic variability, yet quantitative evidence at the local government level remains sparse. This study mapped and quantified LULC change in Daura Local Government Area, Katsina State, over the twenty years from 2006 to 2026. Landsat 7 ETM+, Landsat 8 OLI/TIRS and Landsat 9 OLI/TIRS scenes at 30 m spatial resolution were radiometrically calibrated, atmospherically corrected and segmented using the mean shift algorithm, then classified with an object-based support vector machine into five classes: urban, vegetation, farmland, water bodies and bare land. Classification reliability was assessed against stratified random reference points interpreted from high-resolution imagery. Across the 21,731.4-ha study area, urban land expanded from 581.16 ha (2.67%) to 1,477.87 ha (6.80%), a net gain of 154.3% at a mean annual rate of 4.8%. Vegetation cover rose from 732.68 ha (3.37%) to 1,327.16 ha (6.11%), whilst farmland contracted from 18,606.8 ha (85.62%) to 16,808.6 ha (77.35%), a loss of 1,798.2 ha. Bare land rose to 2,475.8 ha in 2016 before falling to 1,907.96 ha in 2026, and water bodies remained below 1% of the study area throughout. Overall classification accuracy was 81.1%, 89.5% and 96.2% for 2006, 2016 and 2026, with Kappa coefficients of 0.402, 0.723 and 0.889. Conversion of farmland at the urban fringe is the dominant transition, and its pace supports the case for delineating an urban growth boundary and formally protecting irrigated land before the built-up area expands further.

ARTICLE INFORMATION
Received: 15 January 2026
Revised: 29 July 2026
Accepted: 29 July 2026
Published: 30 July 2026

KEYWORDS
Land Use and Land Cover (LULC);
Support Vector Machine (SVM);
spatiotemporal analysis;
Urban expansion;
Daura.

Citation: Olusesi O.C, Usman S. S. & Ngurnoma Y.N. (2026). Geospatial Analysis of Land Use and Land Cover Changes Over Daura, Katsina State. *Journal of Geomatics and Environmental Research*, Special Issue 1(1), Pp 121-139.

1. INTRODUCTION

Land use and land cover (LULC) change is among the clearest measurable expressions of human interaction with the environment, and it operates simultaneously at local, regional and global scales (Turner *et al*., 1995; Winkler *et al*., 2021). Reliable information on how land is being converted, and how quickly, defines development planning, environmental regulation and the allocation of scarce agricultural resources (Olorunfemi *et al*., 2020). In semi-arid West Africa, the question carries additional weight, because the same land supports rainfed cultivation, dry season irrigation, grazing and rapidly growing settlements (Mashala *et al*., 2023). Satellite remote sensing and geographic information systems (GIS) provide the means of measuring these conversions consistently over decades (Campbell & Wynne, 2011). The Landsat and Sentinel Archives are well suited to the task, offering an uninterrupted record at a spatial resolution appropriate to district-level mapping and available without cost (Hussain *et al*., 2022). Recent work has concentrated less on data availability than on classification quality. Dash *et al*. (2023) demonstrated that careful selection of training data and ancillary spectral inputs raises Image classification accuracy substantially in mixed agricultural terrain, whilst Darem *et al*. (2023) reported comparable gains for arid environments in which the spectral separability between bare soil and sparse vegetation is poor.

The support vector machine (SVM), introduced by Cortes and Vapnik (1995), constructs an optimal separating hyperplane between classes in a transformed feature space and performs well where training samples are limited and feature dimensionality is high (Huang *et al*., 2002; Mountrakis *et al*., 2011). Foody and Mathur (2004) showed that the classifier depends more on the quality of the samples lying close to the class boundary than on sample volume, which makes it economical to train. Segmentation-based, or object-based, approaches extend this advantage by classifying homogeneous image objects rather than individual pixels, thereby suppressing the speckle typical of pixel-based products in heterogeneous terrain (Blaschke, 2010). Tan *et al*. (2024) compared random forest and SVM under both pixel-based and object-based schemes and found the object-based configurations more faithful to the true spatial arrangement of cover types, although the two classifiers differed little in overall accuracy. The combination of object-based segmentation with SVM adopted in this study therefore reflects current practice rather than an untested choice.

Nigeria is urbanising quickly. Its urban population is projected to continue expanding well into the middle of the century (United Nations, 2018), and the northern conurbation extending along the axis from Katsina through Kano to Zaria has been identified as one of the fastest growing urban regions in Africa (Bloch *et al*., 2015; Seto *et al*., 2012). Empirical studies across the country describe a consistent pattern. Koko *et al*. (2022) recorded sustained built-up expansion in Kano Metropolis between 1991 and 2020 and projected its continuation to 2050. Onuegbu and Egbu (2024) quantified the loss of 21,000 ha of vegetation to built-up and bare land in Abakaliki between 2000 and 2022, whilst Ologunde *et al*. (2025) reported that roughly half of the built-up expansion in Ado-Odo Ota between 2015 and 2023 came directly from vegetated land. Okeleye *et al*. (2023) linked comparable conversions in the North Central region to migration pressure and declining household food security. What these studies share is a concentration on metropolitan centres and southern states; smaller northern administrative towns have attracted far less attention (Oyedele *et al*., 2023).

Katsina State occupies the transition between the Sudan and Sahel savanna zones, where agricultural expansion, fuelwood extraction and desertification interact (Funtua *et al*., 2019). Daura, one of the seven original Hausa states and the administrative and commercial centre of the surrounding rural district, has grown steadily without a published quantitative account of how that growth has reshaped its immediate hinterland. Aliyu and Amadu (2017) observed that Nigerian urban growth has consistently outpaced the planning instruments intended to guide it, a mismatch that is most acute in towns lacking a current land use inventory. This study addresses that gap for Daura.

The spatial and temporal pattern of LULC change in Daura Local Government Area between 2006 and 2026 is analysed here using multi-temporal Landsat imagery and object-based SVM classification. The specific objectives are to classify and map the distribution of urban land, vegetation cover, farmland, water bodies and bare land for 2006, 2016 and 2026; to quantify the extent and rate of change in each class over the twenty years; to evaluate classification reliability through confusion matrices, overall accuracy and the Kappa coefficient; and to interpret the observed transitions in relation to urban expansion, farmland conversion and land management policy in the study area.

2. MATERIALS AND METHODS

2.1 Software Used

Satellite imagery and supporting literature were downloaded through a standard web browser, and Google Earth Pro was used both to familiarise the analysts with the study area and to supply the high-resolution reference imagery against which the accuracy assessment points were later interpreted. Compressed archives were extracted with WinRAR. Landsat 7 ETM+ scenes acquired after May 2003 contain systematic data gaps caused by failure of the scan line corrector, and these were filled in QGIS before further processing. All subsequent operations, from image clipping and segmentation through classification to accuracy assessment and map production, were carried out in ArcGIS Pro. Microsoft Excel was used to tabulate class areas, compute the change statistics, and generate the trend charts presented in this paper.

2.2 Datasets and Sources

Three Landsat scenes, one for each epoch, together with an administrative boundary layer, constitute the data used in this study. Their characteristics are given in Table 1. Scenes were selected from the late dry season, when cloud cover over northern Katsina is minimal and when the contrast between cultivated land, fallow, and bare surfaces is at its clearest, and each was required to carry less than 10% cloud cover over the study area.

Table 1: *Satellite and ancillary datasets used in the study*

Dataset	Data type	Path/Row	Acquisition date	Resolution	Purpose
Landsat 7 ETM+	Secondary, raster	189/051	2006	30 m	LULC classification, 2006 epoch
Landsat 8 OLI/TIRS	Secondary, raster	189/051	2016	30 m	LULC classification, 2016 epoch
Landsat 9 OLI/TIRS	Secondary, raster	189/051	2026	30 m	LULC classification, 2026 epoch
Administrative boundary	Secondary, vector	Not applicable	Not applicable	1:1,000,000	Delineation and clipping of the study area

3 METHODOLOGY

Figure 1 summarises the sequence of operations followed in this study.

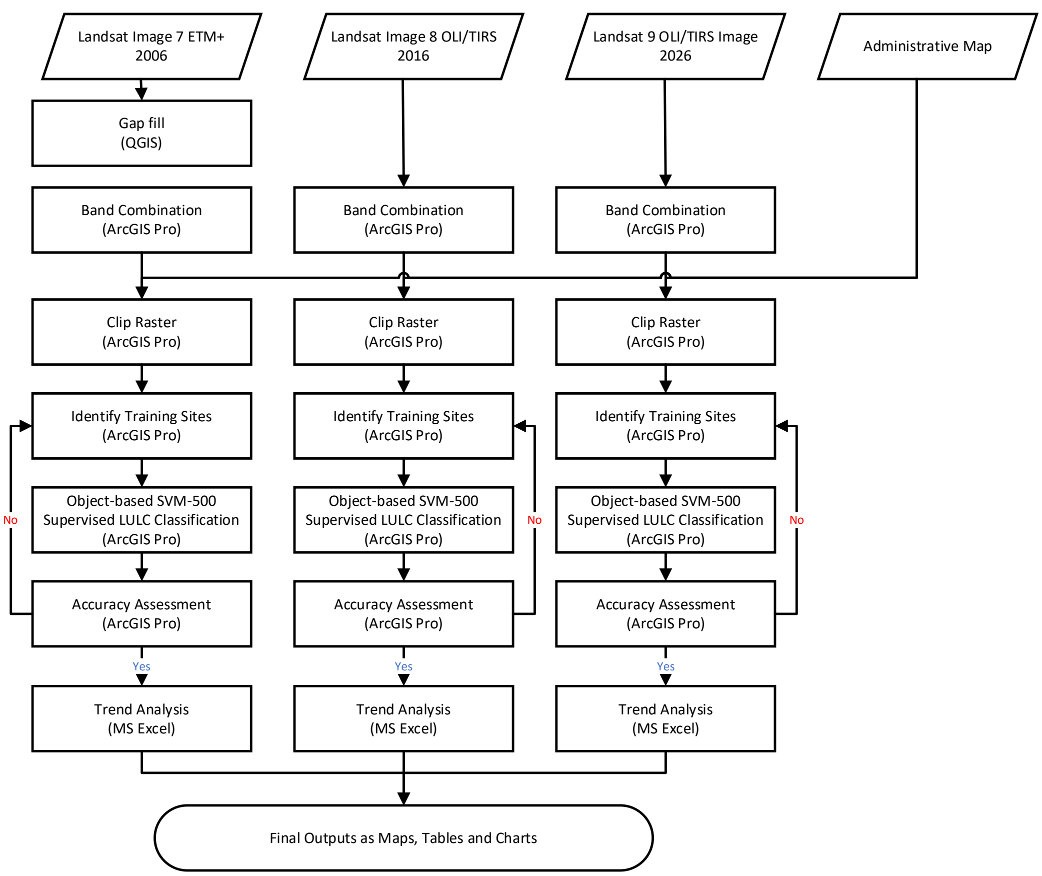

Figure 1. Workflow of the study, from image acquisition and preprocessing through segmentation and classification to accuracy assessment and change analysis.

3.1 Study Area

Daura Local Government Area lies in the northern part of Katsina State, Nigeria, between latitudes 12° 52′ N and 13° 04′ N and longitudes 8° 10′ E and 8° 22′ E and covers approximately 21,731 ha. It is bounded by Mai'adua Local Government Area to the north, Dutsi to the west, and Sandamu to the south and east.

Daura is one of the seven original Hausa Bakwai states and is traditionally recognised as the ancestral home of the Hausa people. The town functions simultaneously as a cultural heritage site and as an administrative centre for the surrounding rural district. Bloch *et al*. (2015) describe the northern Nigerian towns of this belt, among them Katsina, Kano and Sokoto, as historic citadels and political capitals whose early growth was shaped by Saharan and trans-Saharan trade, and whose contemporary expansion now follows a very different logic.

The climate is semi-arid tropical, typical of the Sudan savanna ecological zone. Annual rainfall ranges between 500 and 800 millimetres and is concentrated between June and September, whilst the dry season extends from October to May under the influence of the dry and dusty Harmattan winds from the Sahara. Mean annual temperatures range from 25 °C to 35 °C, with peak values occurring in the hot dry season between March and May. These conditions are shared with other semi-arid areas of northern Nigeria and exert a strong influence on land use patterns and agricultural practice (Funtua *et al*., 2019).

Natural vegetation is predominantly Sudan savanna, consisting of scattered trees, shrubs and grasses adapted to semi-arid conditions. Acacia, baobab and various thorny shrubs are common. This cover has been substantially modified by cultivation, grazing and settlement, and desertification and land degradation remain persistent problems across Katsina State, with vegetation conversion proceeding at appreciable rates (Funtua *et al*., 2019).

Agriculture forms the basis of the local economy, with most of the population engaged in subsistence and commercial farming. Millet, sorghum, groundnuts and cowpeas are the principal crops, supplemented increasingly by irrigated vegetables during the dry season (Funtua *et al*., 2019). Livestock rearing, particularly of cattle, sheep and goats, is also an important activity, and competition between grazing corridors and expanding cultivation has become a documented source of land use conflict in Nigeria (Odiji *et al*., 2024). Agricultural productivity is constrained by erratic rainfall, soil degradation and limited irrigation infrastructure. Comparable pressures have been recorded in the North Central region, where LULC change has been linked directly to migration and to declining household food security (Okeleye *et al*., 2023).

The population of Daura has grown steadily through natural increase and rural to urban migration. As part of the northern conurbation centred on Kano and extending from Katsina to Zaria, the wider region is undergoing some of the most rapid urban expansion in Africa (Bloch *et al*., 2015; Seto *et al*., 2012). This demographic pressure has enlarged the built-up area, raised demand for agricultural land, and intensified the use of natural resources. The town serves as a commercial and administrative hub for the surrounding rural communities, which sustains its continued spatial growth. Figure 2 shows the location of the study area.

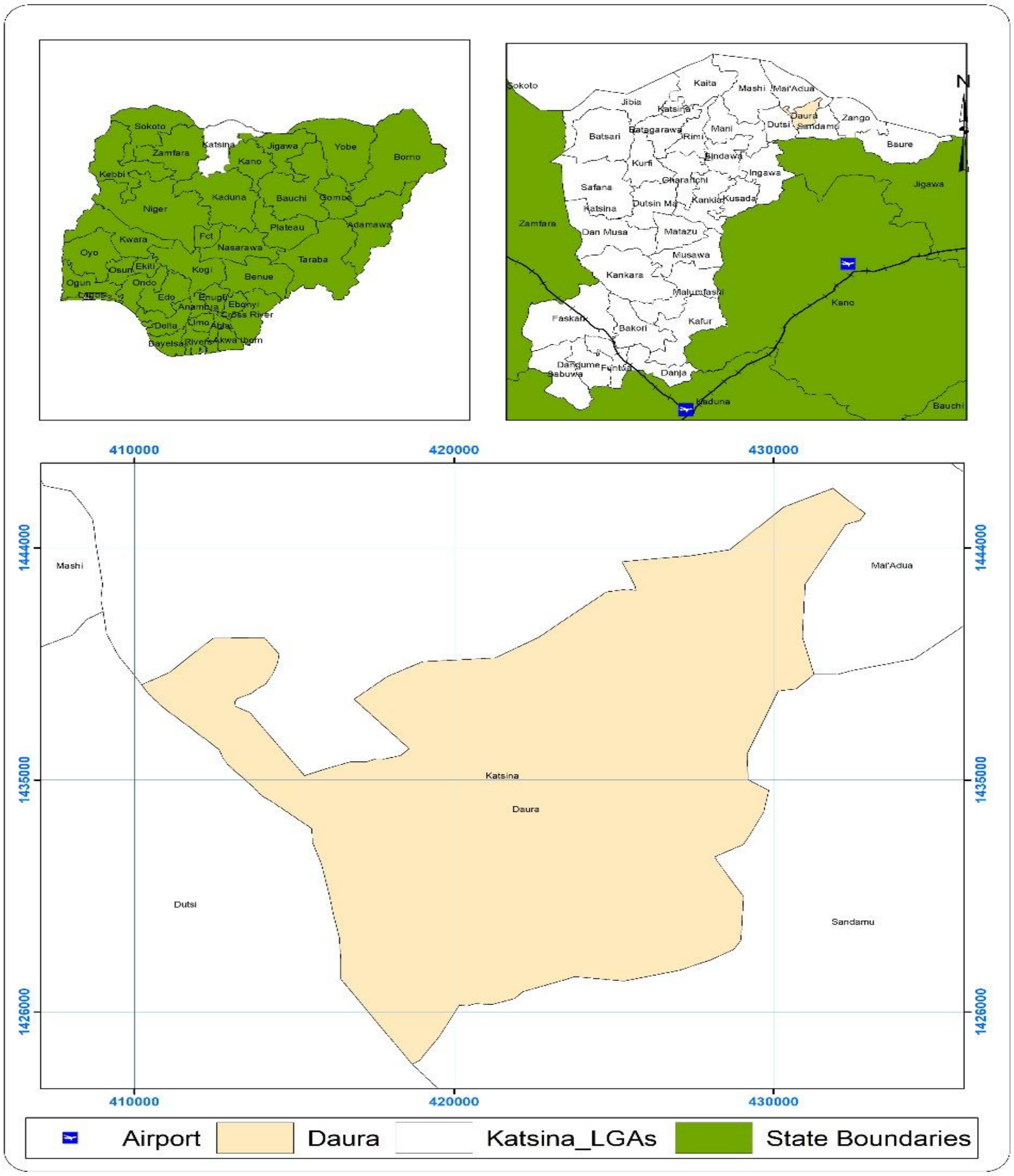

Figure 2. Location of Daura Local Government Area within Katsina State and within Nigeria, with the boundary of the study area shown in the main panel.

3.2 Image Acquisition and Preprocessing

All three Landsat scenes were obtained from the United States Geological Survey EarthExplorer portal. Preprocessing followed a fixed sequence so that the three epochs would be radiometrically comparable.

Digital numbers were first converted to top-of-atmosphere spectral radiance and then to top-of-atmosphere reflectance using the rescaling coefficients and solar geometry supplied in the metadata file accompanying each scene, with a correction for solar zenith angle applied to remove the effect of differing illumination between acquisition dates. Atmospheric correction was then applied using the dark object subtraction method, in which the minimum value observed in each band across the scene is taken to represent the additive path radiance contributed by atmospheric scattering and is subtracted from every pixel in that band (Chavez, 1996).

The Landsat 7 ETM+ scene used for the 2006 epoch was acquired after the failure of the scan line corrector in May 2003 and therefore contains wedge-shaped data gaps that widen towards the edge of the swath and affect approximately 22% of the scene. These gaps were filled in QGIS before classification by interpolating from spectrally similar pixels in the neighbourhood of each gap, a procedure that preserves local spectral structure better than simple linear interpolation. Bands were then stacked into a multispectral composite for each epoch using the visible, near infrared and shortwave infrared bands common to ETM+, OLI and OLI-2, so that the same six-band feature space was presented to the classifier at every epoch; the thermal bands were excluded. Where two scenes were required to cover the study area, they were mosaicked before clipping, with histogram matching applied across the seam. All composites were projected to the Universal Transverse Mercator system, Zone 32 North, on the World Geodetic System 1984 datum, resampled where necessary by nearest neighbour so that original radiometric values were preserved, and clipped to the administrative boundary of Daura Local Government Area.

3.3 Performance Evaluation

Classification was performed on image objects rather than on individual pixels. Each multispectral composite was first partitioned using the mean shift segmentation algorithm (Comaniciu & Meer, 2002) as implemented in ArcGIS Pro, which groups adjacent pixels whose spectral values converge on the same mode into a single segment. Three parameters govern the outcome, and identical values were applied at all three epochs so that segment geometry would not vary systematically between dates: spectral detail was set to 15.5 on the 1 to 20 scale, spatial detail to 15, and the minimum segment size to 20 pixels, equivalent to 1.8 ha on the ground. The relatively high spectral detail setting was needed to separate built-up surfaces from bare land, which are spectrally similar in this environment, whilst the minimum segment size was chosen to suppress fragmentation of the extensive farmland matrix without dissolving the smaller residential blocks at the edge of the town.

Five classes were defined for the study area, following the cover types that could be reliably separated at 30 m resolution. Their definitions are set out in Table 2.

Table 2. Definition of the land use and land cover classes

Class	Definition
Urban	Built-up surfaces, including residential and commercial buildings, compounds, roads and other impervious or heavily compacted surfaces associated with settlement.
Vegetation	Natural and planted woody cover, including scattered trees, shrubland, riparian vegetation and orchards, together with perennial grassland retaining cover through the dry season.
Farmland	Land under rainfed or irrigated cultivation, including harvested and fallow fields that retain visible field boundaries and crop residue.
Water bodies	Permanent and seasonal open water, including reservoirs, ponds, dams and channels holding water at the time of image acquisition.
Bare land	Exposed soil, sand and rock without discernible vegetation cover or cultivation, including degraded surfaces, borrow pits and quarry sites.

Training segments were delineated on screen by reference to the false colour composite and to Google Earth imagery of the corresponding year. A minimum of 30 training segments per class per epoch was collected, distributed across the study area rather than clustered, so that within-class spectral variability was adequately represented.

The segments were classified using a support vector machine with a radial basis function kernel. The maximum number of training samples drawn per class was set to 500, the setting from which the abbreviation SVM-500 used in this paper derives; where a class contained fewer than 500 candidate samples, all available samples were used. Eight segment attributes were supplied to the classifier, namely the mean digital number and the standard deviation of each of the converged colour bands, together with the count of pixels, the compactness and the rectangularity of each segment. Classification proceeded iteratively. Where the resulting map showed visible confusion between classes, the training segments responsible were edited or replaced, and the classifier was retrained, and this cycle was repeated until overall accuracy exceeded 80% and no systematic misassignment remained on visual inspection.

3.4 Accuracy Assessment

Classification accuracy was assessed independently for each epoch using a stratified random sample of reference points generated in ArcGIS Pro, with the sample allocated across classes in proportion to their mapped extent subject to a minimum allocation per class, so that classes of small extent such as water bodies would still be represented. Approximately 300 points were generated per epoch; after the removal of points falling outside the study boundary or on ambiguous surfaces, 307 points were retained for 2006 and 314 for each of 2016 and 2026. Figure 3 shows their distribution.

Each point was interpreted against the highest resolution imagery available for the corresponding year in Google Earth Pro, supplemented by the field knowledge of the authors, who have worked in the study area. Interpretation was carried out without reference to the classified map to avoid confirmation bias.

The resulting confusion matrices report the classified class as rows and the reference class as columns. User's accuracy, the proportion of segments assigned to a class that were correctly assigned, was computed for each row, and producer's accuracy, the proportion of reference points of a class that the classifier captured, was computed for each column. Overall accuracy is the proportion of all reference points correctly classified, and the Kappa coefficient expresses the improvement of the classification over the agreement expected by chance (Foody, 2002). Kappa values were interpreted against the benchmarks of Landis and Koch (1977), under which values between 0.41 and 0.60 indicate moderate agreement, values between 0.61 and 0.80 substantial agreement, and values above 0.80 almost perfect agreement.

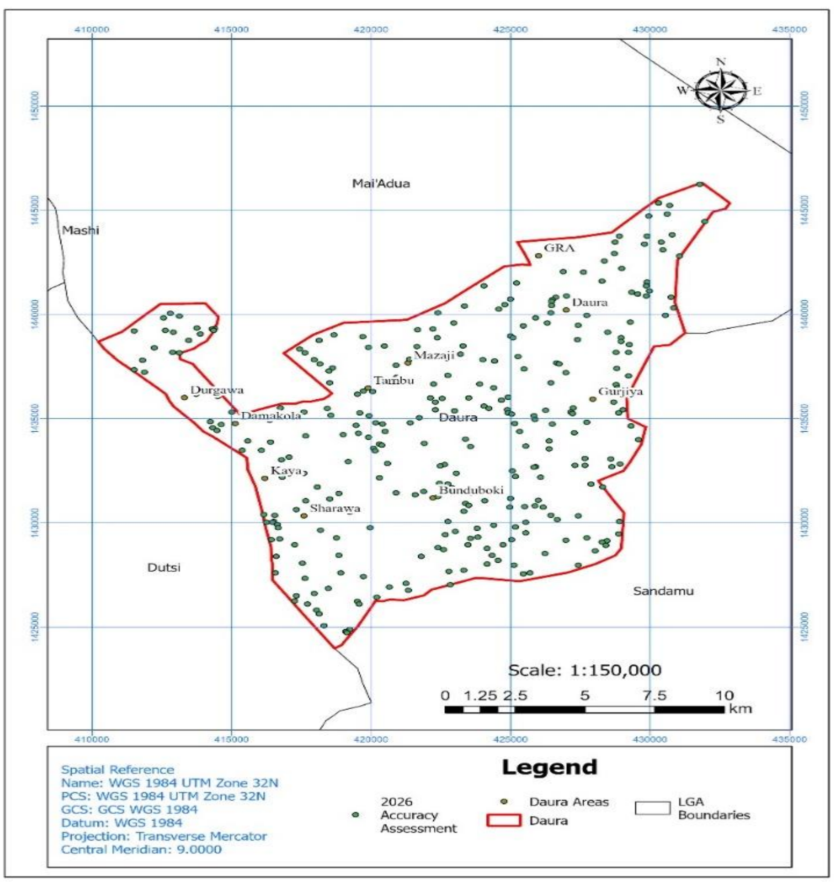

Figure 3. Distribution of the stratified random reference points used for accuracy assessment, shown against the classified land cover of the study area.

3.5 Change Detection and Trend Analysis

Class areas were extracted for each epoch and expressed in hectares and as percentages of the total study area. Change was quantified by post-classification comparison, in which the independently classified maps for the three epochs are compared class by class. This approach was preferred to spectral change detection because it is insensitive to residual radiometric differences between sensors and because it yields directly interpretable class-to-class statistics (Onuegbu & Egbu, 2024). Net change was computed as the difference in area between successive epochs, percentage change was expressed relative to the earlier epoch, and the mean annual rate of change was computed as the compound rate that carries the earlier area to the later area over the intervening period.

4. RESULTS AND DISCUSSION

4.1 LULC Distribution

Figures 4 to 6 present the classified maps for 2006, 2016 and 2026. Farmland dominates the study area at every epoch and forms a continuous matrix within which the other classes are embedded. Urban land occupies a compact core at the centre of the local government area corresponding to Daura town, and the sequence of maps shows this core thickening and extending outwards along the roads radiating from it rather than appearing as new detached settlements. Vegetation is concentrated in the northern and eastern parts of the area and along drainage lines. Bare land is more dispersed, occurring as patches within the farmland matrix, and its distribution shifts noticeably between epochs.

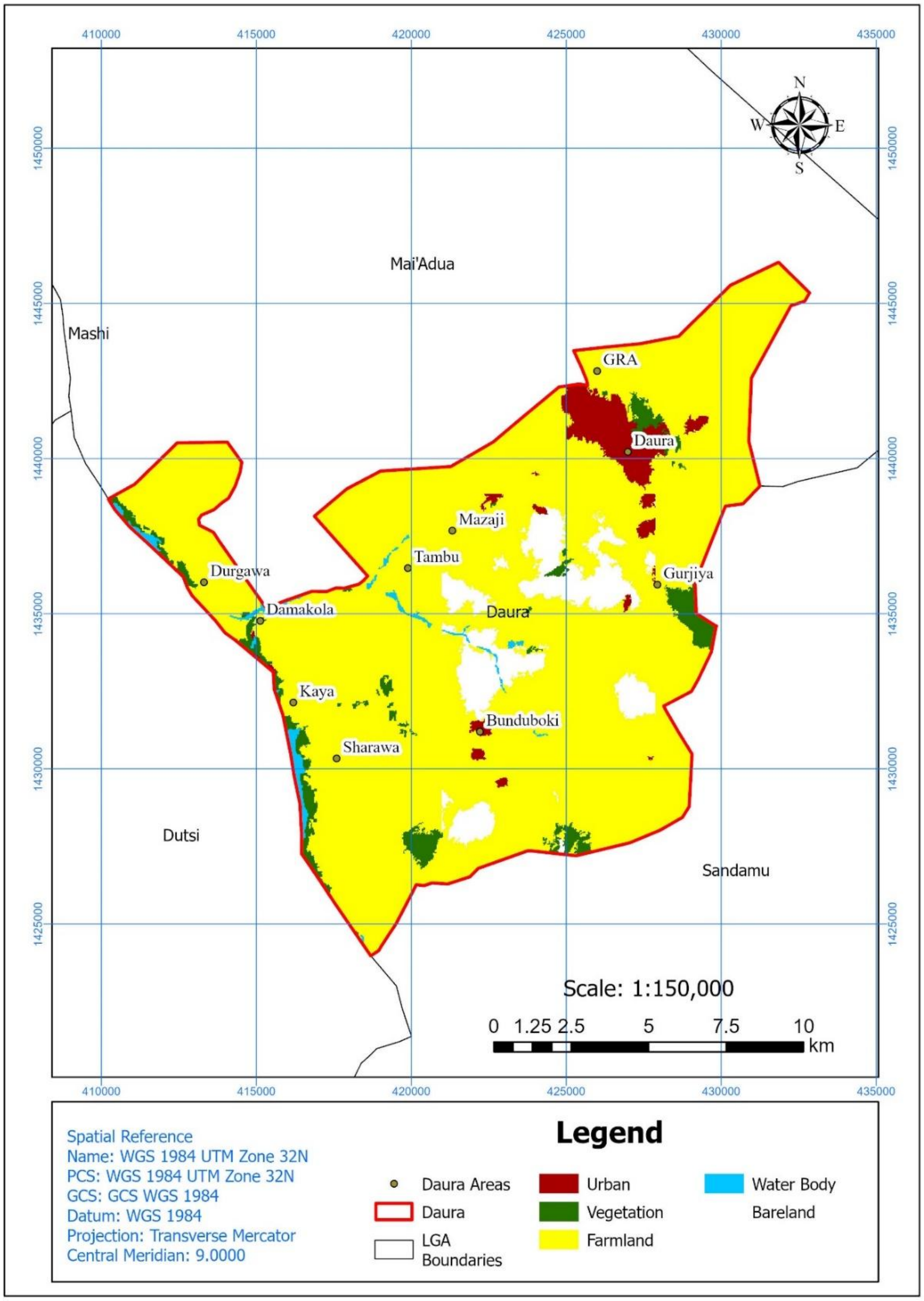

Figure 4. Land use and land cover of Daura Local Government Area in 2006, classified from Landsat 7 ETM+ imagery using object-based support vector machine classification.

ISSN 2682-681X (Paper), ISSN 2705-4241 (Online) | http://unilorinjoger.com | https://doi.org/10.63745/jogersi.2026.06.30.009

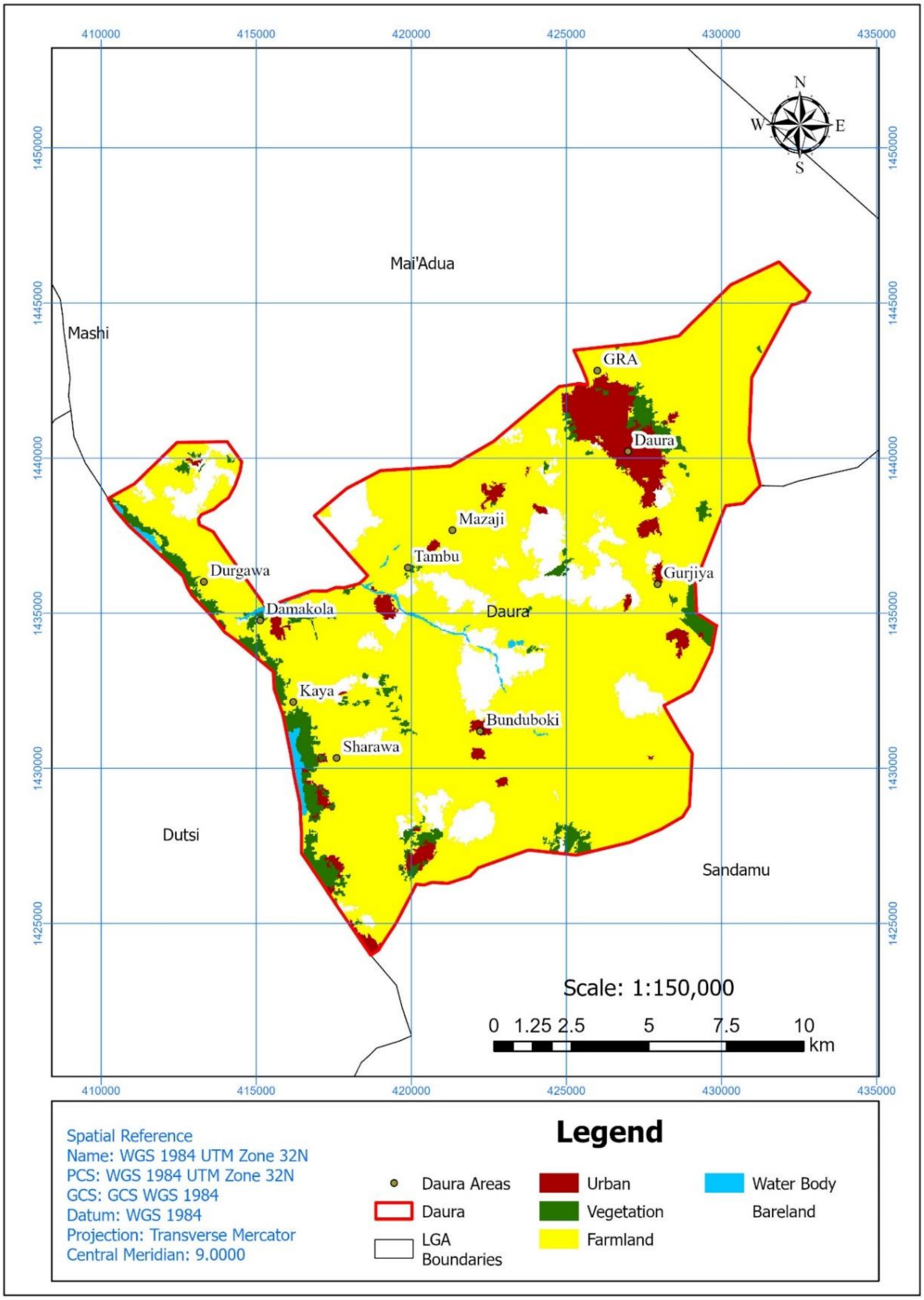

Figure 5. Land use and land cover of Daura Local Government Area in 2016, classified from Landsat 8 OLI/TIRS imagery using object-based support vector machine classification.

ISSN 2682-681X (Paper), ISSN 2705-4241 (Online) | http://unilorinjoger.com | https://doi.org/10.63745/jogersi.2026.06.30.009

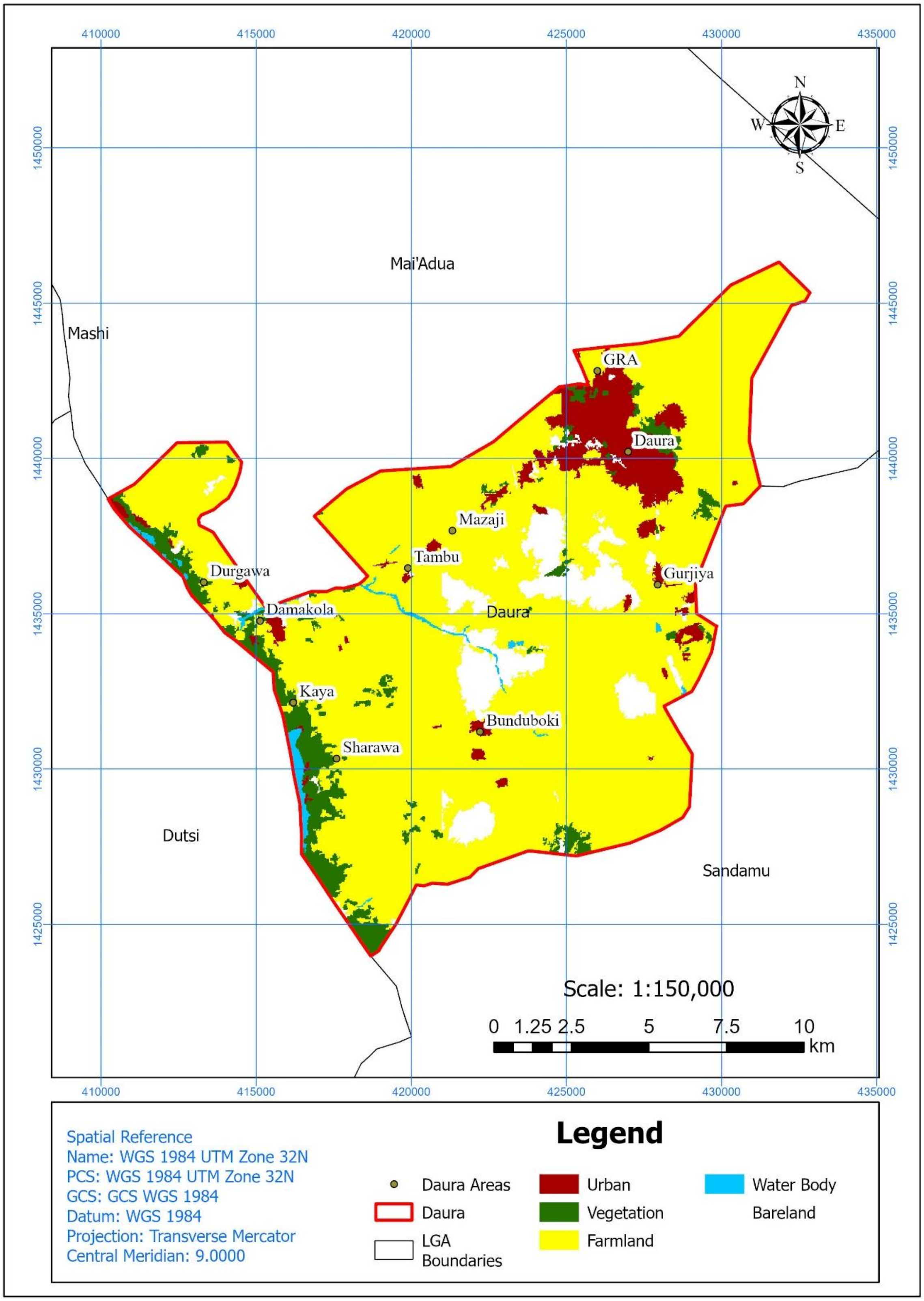

Figure 6. Land use and land cover of Daura Local Government Area in 2026, classified from Landsat 9 OLI/TIRS imagery using object-based support vector machine classification.

4.2 Trend Analysis

Table 3 presents the area and proportion of each class at the three epochs, together with the change recorded between successive epochs. The total mapped area is constant at 21,731.4 ha.

Table 3. *Land use and land cover distribution over Daura Local Government Area, 2006 to 2026*

Class	2006 area (ha)	%	2016 area (ha)	%	Change 2006 to 2016 (ha)	2026 area (ha)	%	Change 2016 to 2026 (ha)
Urban	581.16	2.67	1,075.13	4.95	+493.97	1,477.87	6.80	+402.74
Vegetation	732.68	3.37	1,110.94	5.11	+378.26	1,327.16	6.11	+216.22
Farmland	18,606.80	85.62	16,882.70	77.69	-1,724.10	16,808.60	77.35	-74.10
Water bodies	189.94	0.87	186.79	0.86	-3.15	209.74	0.97	+22.95
Bare land	1,620.75	7.46	2,475.80	11.39	+855.05	1,907.96	8.78	-567.84
Total	21,731.40	100.00	21,731.40	100.00		21,731.40	100.00	

Urban land increased at every interval, from 581.16 ha in 2006 to 1,075.13 ha in 2016 and 1,477.87 ha in 2026. The net gain of 896.71 ha represents an increase of 154.3% on the 2006 extent, equivalent to a mean annual growth rate of 4.8%. Growth was faster in the first decade, when urban land expanded by 85.0%, than in the second, when it expanded by 37.5%.

Farmland declined throughout the period, from 18,606.8 ha to 16,808.6 ha, a net loss of 1,798.2 ha or 9.7% of its 2006 extent. Almost all of that loss occurred between 2006 and 2016, when farmland fell by 1,724.1 ha; the further decline between 2016 and 2026 amounted to only 74.1 ha.

Vegetation cover rose from 732.68 ha to 1,327.16 ha, a gain of 81.1%, again concentrated in the first decade. Bare land followed a non-monotonic path, rising by 855.05 ha to 2,475.8 ha in 2016 and then falling by 567.84 ha to 1,907.96 ha in 2026. Water bodies varied within a narrow band, from 189.94 ha in 2006 to 186.79 ha in 2016 and 209.74 ha in 2026, and at no epoch exceeded 1% of the study area. Figures 7 to 9 present these patterns graphically.

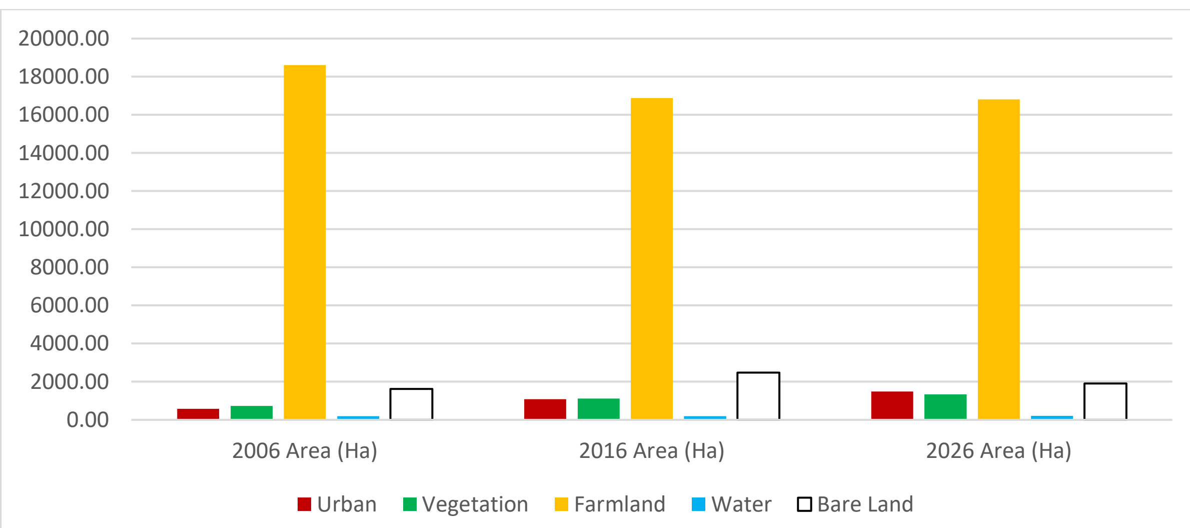

Figure 7. Area occupied by each land use and land cover class in 2006, 2016 and 2026, in hectares.

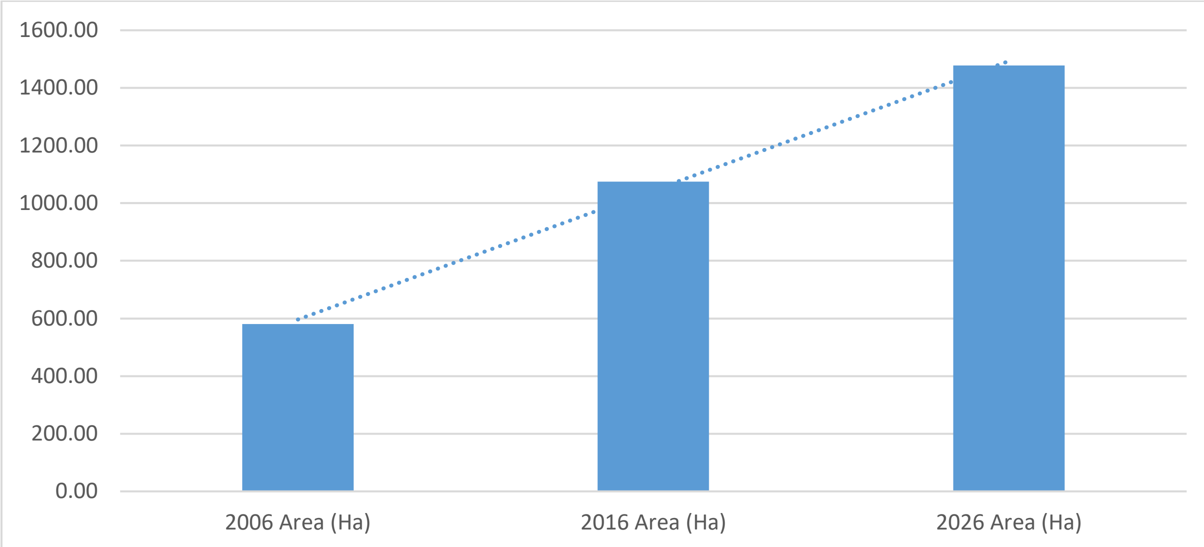

Figure 8. Growth of urban land in Daura Local Government Area between 2006 and 2026, in hectares.

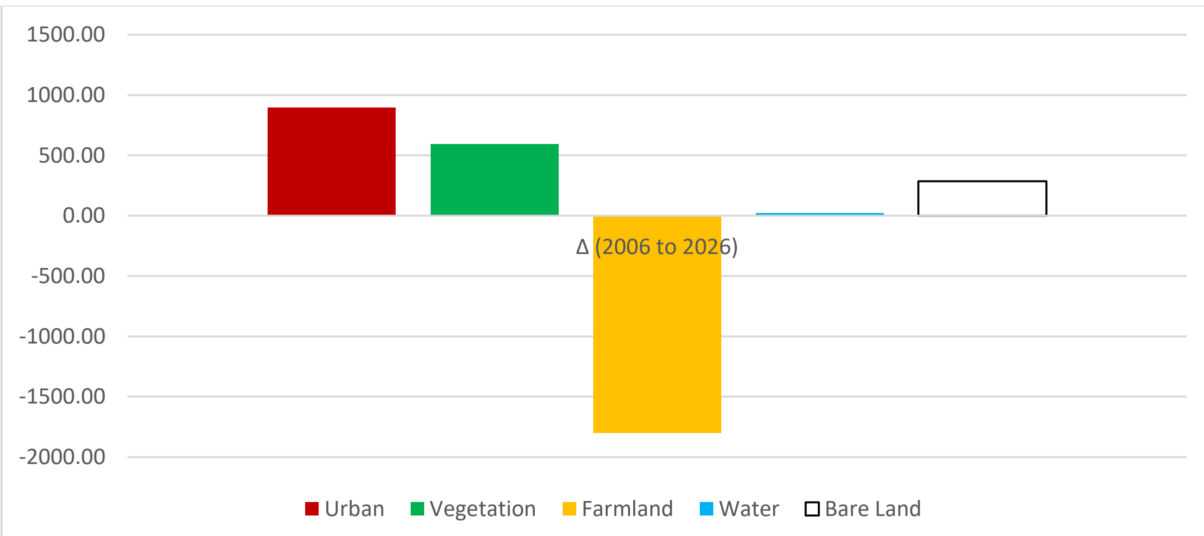

Figure 9. Net change in the area of each land use and land cover class between 2006 and 2026, in hectares. Positive values denote gain and negative values denote loss.

4.3 Classification Accuracy

Tables 4 to 6 present the confusion matrices for the three epochs. Overall accuracy rose from 81.1% in 2006 to 89.5% in 2016 and 96.2% in 2026, with corresponding Kappa coefficients of 0.402, 0.723 and 0.889.

Table 4: *Confusion matrix for the object-based classification of the 2006 image*

Classified class	Urban	Vegetation	Farmland	Water	Bare land	Total	User's accuracy (%)
Urban	19	1	0	0	0	20	0.95
Vegetation	1	13	2	1	1	18	0.722
Farmland	4	9	232	8	3	256	0.906
Water bodies	0	0	0	10	0	10	1
Bare land	2	1	0	0	7	10	0.7
Total	26	24	234	19	11	314	0
Producer's accuracy (%)	0.731	0.542	0.991	0.526	0.636	0	0.895

Overall accuracy = 81.1%; Kappa coefficient = 0.402.

Table 5. *Confusion matrix for the object-based classification of the 2016 image*

Classified class	Urban	Vegetation	Farmland	Water	Bare land	Total	User's accuracy (%)
Urban	8	0	0	0	0	8	1
Vegetation	1	7	2	0	0	10	0.7
Farmland	12	8	226	2	33	281	0.804
Water bodies	0	0	0	8	0	8	1
Bare land	0	0	0	0	0	0	0
Total	21	15	228	10	33	307	0
Producer's accuracy (%)	0.381	0.467	0.991	0.8	0	0	0.811

Overall accuracy = 89.5%; Kappa coefficient = 0.723.

Table 6. *Confusion matrix for the object-based classification of the 2026 image*

Classified class	Urban	Vegetation	Farmland	Water	Bare land	Total	User's accuracy (%)
Urban	19	1	0	0	0	20	95.0
Vegetation	0	16	1	1	0	18	88.9
Farmland	1	3	248	2	2	256	96.9
Water bodies	0	0	0	10	0	10	100.0
Bare land	0	1	0	0	9	10	90.0
Total	20	21	249	13	11	314	
Producer's accuracy (%)	95.0	76.2	99.6	76.9	81.8		96.2

Overall accuracy = 96.2%; Kappa coefficient = 0.889.

Farmland accounted for 281 of the 307 reference points in the 2006 accuracy assessment, so a high overall accuracy could be attained without discriminating against the remaining classes well, and Kappa penalizes precisely this. Bare land was not identified at all in 2006: all 33 reference points belonging to that class were assigned to farmland, giving a producer's accuracy of zero. Producer's accuracies for urban and vegetation were also low, at 38.1% and 46.7% respectively.

Class-level performance improves markedly at the later epoch. By 2026, producers' accuracy exceeded 76% for every class and user's accuracy exceeded 88%, and the residual confusion is confined to a small number of vegetation and water points assigned to farmland. This improvement tracks the improving radiometric quality of the sensors across the series, from the gap-affected ETM+ scene through OLI to OLI-2.

5. DISCUSSION

Over twenty years, the land surface of Daura moved decisively in one direction. Built-up land expanded, farmland contracted, and the exchange between the two was concentrated at the edge of the town. The magnitude of that exchange is instructive: urban land gained 896.71 ha whilst farmland lost 1,798.2 ha, which means that farmland was not converted to urban use alone. Vegetation and bare land together gained

881.7 ha over the same period, accounting almost exactly for the residual, so roughly half of the farmland lost passed into these two classes rather than into settlement.

The urban growth rate observed here, 4.8% per annum compounded, sits within the range reported for comparable Nigerian settlements but towards its lower end. Koko *et al*. (2022) documented sustained built-up expansion in Kano Metropolis, the dominant centre of the conurbation in which Daura sits, between 1991 and 2020. In Nguru, a town of similar administrative rank in neighbouring Yobe State, built-up area rose from 446 ha in 2001 to 2,483 ha in 2021 (Yusuf, 2023), a far steeper trajectory than the one recorded here. Onuegbu and Egbu (2024) reported 7,500 ha of built-up gain in Abakaliki between 2000 and 2022, and Ologunde *et al*. (2025) recorded 138.2 km² of built-up gain in Ado-Odo Ota over only eight years. Daura is therefore expanding, but from a small base and at a moderate pace by national standards, which is consistent with its position as a district centre rather than a metropolitan node.

Attributing this expansion requires care. Bloch *et al*. (2015) argued that natural increase within existing urban populations, rather than rural to urban migration, is the principal component of Nigerian urban growth, a conclusion that shifts the policy emphasis from controlling migration towards accommodating a population that is already present. The administrative function of Daura as a local government headquarters, its commercial role as a market centre for the surrounding rural district, and its proximity to the border trade route with the Niger Republic all contribute additional demand for built land. The spatial signature of the growth supports this reading, since expansion is contiguous with the existing built-up core and follows the road network rather than appearing as detached speculative development, a pattern characteristic of demand generated locally rather than by external investment.

The loss of 1,798.2 ha of farmland, 9.7% of the 2006 extent, is significant in a district where agriculture is the principal livelihood. Its timing is revealing: 1,724.1 ha were lost between 2006 and 2016 against only 74.1 ha between 2016 and 2026. Two readings are possible. One is that conversion pressure eased after 2016. The other, which the bare land figures support, is that the earlier decade saw a large area of marginal farmland abandoned or degraded rather than built upon, and that what continued after 2016 was the slower but more permanent conversion of productive land to built-up use. Farmland losses of this kind have been linked to declining household food security elsewhere in Nigeria (Okeleye *et al*., 2023), and the concern in Daura is sharpened by the fact that the land nearest the town, which is under the greatest conversion pressure, is also the land most likely to be irrigated in the dry season.

The increase in vegetation cover, from 732.68 ha to 1,327.16 ha, runs counter to the regional narrative of progressive desertification and deserves careful interpretation rather than uncritical acceptance. Three explanations are plausible, and they are not mutually exclusive. The first is genuine woody cover gain through shelterbelt planting, farmer-managed natural regeneration and the expansion of irrigated tree crops around the town, all of which have been promoted in the dryland states. The second is redistribution rather than creation: the same decade in which vegetation rose by 378.26 ha saw bare land rise by 855.05 ha and farmland fall by 1,724.1 ha, a combination consistent with cultivated land passing out of production into fallow, where regenerating shrub cover is spectrally difficult to distinguish from established vegetation at 30 m resolution. The third explanation is methodological. The 2006 classification failed to detect bare land, and although vegetation user's accuracy at that epoch was 70.0%, its producer's accuracy was only 46.7%, so the 2006 vegetation extent is likely to be underestimated, which would inflate the apparent gain. Separating these explanations would require either multi-season imagery, which distinguishes perennial woody cover from seasonally green fallow, or a vegetation index time series, and neither fell within the scope of this study. The finding is therefore reported as a measured increase in dry season green cover rather than as evidence of ecological recovery.

Bare land rose by 855.05 ha between 2006 and 2016 and then fell by 567.84 ha by 2026. The rise coincides almost exactly with the period of steepest farmland loss, which supports the reading of that loss as abandonment and degradation rather than construction, since land clearing, exhaustion of soil fertility and removal of vegetative cover all expose soil, and these processes are documented across Katsina State (Funtua *et al*., 2019). The subsequent fall is more ambiguous. It may reflect re-cultivation following better rainfall, absorption of bare surfaces into the expanding built-up area, or the effect of soil conservation and shelterbelt work. Because the 2006 classification did not detect bare land at all, the 2006 baseline for this class is itself uncertain, and the magnitude of the initial rise should be treated with corresponding caution.

Water bodies remained below 1% of the study area throughout, varying only between 186.79 ha and 209.74 ha. This apparent stability should not be read as evidence of a secure water supply. Single-date dry season imagery captures only the water present on the day of acquisition, and in a Sudan savanna environment, seasonal ponds and channels that carry substantial water in September are dry by March, so the class as mapped approximates permanent water rather than total water availability. Its small extent nonetheless constrains what is possible: with under 210 ha of open water serving both an expanding town and dry season irrigation, competition between urban and agricultural demand is a more likely source of future conflict than absolute scarcity.

The accuracy achieved, between 81.1% and 96.2% overall, is comparable with recent Landsat-based work in Nigeria and elsewhere. Onuegbu and Egbu (2024) reported 95% and 97% for two epochs in Abakaliki, and Ologunde *et al*. (2025) reported 83.3% and 84.1% for Ado-Odo Ota. The upward trend across the Daura series reflects sensor improvement more than analyst improvement, since the 2006 result rests on gap-filled ETM+ data whereas the 2026 result uses OLI-2, which offers higher radiometric resolution and better signal-to-noise performance. The choice of an object-based rather than a pixel-based approach is supported by Tan *et al*. (2024), who found object-based configurations produced more realistic cover distributions, and the performance of SVM under limited training data is consistent with Huang *et al*. (2002), Foody and Mathur (2004), and the review of Mountrakis *et al*. (2011). The disparity between overall accuracy and Kappa in 2006 nevertheless illustrates a general point about accuracy reporting in areas dominated by a single class. Overall accuracy alone would have presented that classification as acceptable, and only the Kappa coefficient and the class-level producer's accuracies reveal that four of the five classes were poorly resolved.

5.1 Implications for Land Use Planning and Environmental Management

The results carry four practical consequences for land administration in Daura. The direction of urban growth is as informative as its magnitude. Expansion has been contiguous and corridor-following rather than dispersed, which means it remains tractable through conventional development control. Delineating and gazetting an urban growth boundary now, whilst the built-up area occupies less than 7% of the local government area, would be considerably cheaper than retrofitting services to scattered settlement later. Koko *et al*. (2022) reached a similar conclusion for Kano, where the window for such intervention has largely closed.

Farmland loss is concentrated at the urban fringe, which is also where soils are most intensively worked and where dry season irrigation is practised. Blanket agricultural land protection is neither realistic nor desirable in a growing town but designating the irrigated fadama areas as land unavailable for conversion would protect the most productive fraction at limited cost to the urban land supply. The connection between such conversions and household food security is now well documented in Nigeria (Okeleye *et al*., 2023).

The volatility of bare land, which rose by more than half in one decade and then fell in the next, indicates that a substantial area is moving in and out of production. This land is the appropriate target for restoration investment, since recovering land that has already been cleared avoids the opportunity cost of restricting land currently under cultivation.

Finally, the study establishes a quantitative baseline where none previously existed, and its value depends on repetition. Reclassifying the same area at five-yearly intervals using the same class definitions and the same classifier would convert a single measurement into a monitoring series capable of detecting whether any of the interventions above are taking effect.

5.2 Limitations of the Study

Three limitations qualify these findings. The 2006 classification rests on a gap-filled Landsat 7 ETM+ scene and returned a Kappa coefficient of 0.402, indicating only moderate agreement beyond chance, so the 2006 class areas, particularly for bare land and vegetation, are the least reliable in the series. Single-date imagery also cannot separate permanent vegetation from seasonally green fallow in a Sudan savanna environment, which means the vegetation and farmland classes are not fully independent of one another. Lastly, the study quantifies change without modelling it: the drivers advanced above are inferred from the spatial pattern of change and from the regional literature rather than tested against demographic, economic or climatic data. Coupling the classification presented here with such data, or with a cellular automata and Markov chain projection of the kind applied by Koko *et al*. (2022), would allow the trajectory to be extended forward rather than only described.

4. CONCLUSION AND RECOMMENDATIONS

Between 2006 and 2026, the land surface of Daura Local Government Area changed in a direction that is consistent across all three epochs measured. Urban land grew by 154.3%, from 581.16 ha to 1,477.87 ha, at a mean annual rate of 4.8%, and it did so by extending outwards from an existing core along established road. Farmland fell by 1,798.2 ha, from 85.62% to 77.35% of the study area, with most of that loss occurring in the first decade. Vegetation cover rose by 81.1%, bare land rose and then fell, and water bodies remained a marginal component of the area throughout. Object-based support vector machine classification reproduced these patterns with overall accuracies of 81.1%, 89.5% and 96.2% and Kappa coefficients of 0.402, 0.723 and 0.889, the weakest performance being associated with the gap-affected 2006 imagery.

The transition that matters for policy is the conversion of farmland at the edge of Daura town into built-up land. It is proceeding steadily, it is spatially concentrated, and it is at present still small enough in absolute terms to be managed.

Four recommendations follow. The Katsina State Ministry of Land and Physical Planning, working with Daura Local Government, should delineate and gazette an urban growth boundary that directs expansion onto land of low agricultural value and away from the irrigated fadama. Land currently under dry season irrigation should be surveyed and formally designated as protected agricultural land. The bare land identified in this study, much of which appears to be degraded former farmland, should be prioritised for shelterbelt planting and soil conservation works in preference to clearing additional land for the same purpose. The classification presented here should also be repeated at five-year intervals using identical class definitions, so that the effect of any intervention can be measured against the baseline established in this paper.

Future work should extend the analysis in two directions: the use of multi-season or vegetation index composites to separate perennial woody cover from seasonal fallow, and the integration of population, rainfall and land price data into a predictive model capable of projecting the Daura land surface forward to 2040.

REFERENCES

Aliyu, A., & Amadu, L. (2017). Urbanization, cities, and health: The challenges to Nigeria: A review. *Annals of African Medicine, 16*(4), 149–158. https://doi.org/10.4103/aam.aam_1_17

Blaschke, T. (2010). Object-based image analysis for remote sensing. *ISPRS Journal of Photogrammetry and Remote Sensing, 65*(1), 2–16. https://doi.org/10.1016/j.isprsjprs.2009.06.004

Bloch, R., Fox, S., Monroy, J., & Ojo, A. (2015). *Urbanisation and urban expansion in Nigeria*. Urbanisation Research Nigeria, ICF International.

Campbell, J. B., & Wynne, R. H. (2011). *Introduction to remote sensing* (5th ed.). The Guilford Press.

Chavez, P. S. (1996). Image-based atmospheric corrections: Revisited and improved. *Photogrammetric Engineering and Remote Sensing, 62*(9), 1025–1036.

Comaniciu, D., & Meer, P. (2002). Mean shift: A robust approach toward feature space analysis. *IEEE Transactions on Pattern Analysis and Machine Intelligence, 24*(5), 603–619. https://doi.org/10.1109/34.1000236

Cortes, C., & Vapnik, V. (1995). Support-vector networks. *Machine Learning, 20*(3), 273–297. https://doi.org/10.1007/BF00994018

Darem, A. A., Alhashmi, A. A., Almadani, A. M., Alanazi, A. K., & Sutantra, G. A. (2023). Development of a map for land use and land cover classification of the Northern Border Region using remote sensing and GIS. *The Egyptian Journal of Remote Sensing and Space Science, 26*(2), 341–350. https://doi.org/10.1016/j.ejrs.2023.04.005

Dash, P., Sanders, S. L., Parajuli, P., & Ouyang, Y. (2023). Improving the accuracy of land use and land cover classification of Landsat data in an agricultural watershed. *Remote Sensing, 15*(16), 4020. https://doi.org/10.3390/rs15164020

Foody, G. M. (2002). Status of land cover classification accuracy assessment. *Remote Sensing of Environment, 80*(1), 185–201. https://doi.org/10.1016/S0034-4257(01)00295-4

Foody, G. M., & Mathur, A. (2004). Toward intelligent training of supervised image classifications: Directing training data acquisition for SVM classification. *Remote Sensing of Environment, 93*(1–2), 107–117. https://doi.org/10.1016/j.rse.2004.06.017

Funtua, A. I., Musa, H., & Babayo, A. (2019). Analysis of land use/land cover changes in Katsina State, Nigeria. *International Journal of Advanced Research and Publications, 3*(8), 21–28.

Huang, C., Davis, L. S., & Townshend, J. R. G. (2002). An assessment of support vector machines for land cover classification. *International Journal of Remote Sensing, 23*(4), 725–749. https://doi.org/10.1080/01431160110040323

Hussain, S., Mubeen, M., & Karuppannan, S. (2022). Land use and land cover (LULC) change analysis using TM, ETM+ and OLI Landsat images in district of Okara, Punjab, Pakistan. *Physics and Chemistry of the Earth, 126*, 103117.

Koko, A. F., Han, Z., Wu, Y., Abubakar, G. A., & Bello, M. (2022). Spatiotemporal land use/land cover mapping and prediction based on hybrid modeling approach: A case study of Kano Metropolis, Nigeria (2020–2050). *Remote Sensing, 14*(23), 6083. https://doi.org/10.3390/rs14236083

Landis, J. R., & Koch, G. G. (1977). The measurement of observer agreement for categorical data. *Biometrics, 33*(1), 159–174. https://doi.org/10.2307/2529310

Mashala, M. J., Dube, T., Mudereri, B. T., Ayisi, K. K., & Ramudzuli, M. R. (2023). A systematic review on advancements in remote sensing for assessing and monitoring land use and land cover changes impacts on surface water resources in semi-arid tropical environments. *Remote Sensing, 15*(16), 3926. https://doi.org/10.3390/rs15163926

Mountrakis, G., Im, J., & Ogole, C. (2011). Support vector machines in remote sensing: A review. *ISPRS Journal of Photogrammetry and Remote Sensing, 66*(3), 247–259. https://doi.org/10.1016/j.isprsjprs.2010.11.001

Odiji, C. A., Ahmad, H. S., Adepoju, M. O., Odia, B., Hamza, D. D., & Akpabio, W. E. (2024). Analysis and prediction of land use/land cover changes and its impacts on the corridors of cattle grazing routes in Benue State, Nigeria. *Geology, Ecology, and Landscapes, 8*(5), 498–512. https://doi.org/10.1080/24749508.2022.2154929

Okeleye, S. O., Okhimamhe, A. A., Sanfo, S., & Fürst, C. (2023). Impacts of land use and land cover changes on migration and food security of North Central Region, Nigeria. *Land, 12*(5), 1012. https://doi.org/10.3390/land12051012

Ologunde, O. H., Kelani, M. O., Biru, M. K., Olayemi, A. B., & Nunes, M. R. (2025). Land use and land cover changes: A case study in Nigeria. *Land, 14*(2), 389. https://doi.org/10.3390/land14020389

Olorunfemi, I. E., Fasinmirin, J. T., Olufayo, A. A., & Komolafe, A. A. (2020). GIS and remote sensing-based analysis of the impacts of land use/land cover change (LULCC) on the environmental sustainability of Ekiti State, southwestern Nigeria. *Environment, Development and Sustainability, 22*(2), 661–692.

Onuegbu, F. E., & Egbu, A. U. (2024). Employing post classification comparison to detect land use cover change patterns and quantify conversions in Abakaliki LGA Nigeria from 2000 to 2022. *Scientific Reports, 14*, 9384. https://doi.org/10.1038/s41598-024-59056-w

Oyedele, A. A., Omosekeji, A. E., Oyedele, K., & Oyedele, T. (2023). Spatio-temporal analysis of land use/land cover dynamics in Abeokuta and environs, southwestern Nigeria. *GeoJournal, 88*(6), 5815–5824. https://doi.org/10.1007/s10708-023-10943-1

Seto, K. C., Güneralp, B., & Hutyra, L. R. (2012). Global forecasts of urban expansion to 2030 and direct impacts on biodiversity and carbon pools. *Proceedings of the National Academy of Sciences, 109*(40), 16083–16088. https://doi.org/10.1073/pnas.1211658109

Tan, Y.-C., Duarte, L., & Teodoro, A. C. (2024). Comparative study of random forest and support vector machine for land cover classification and post-wildfire change detection. *Land, 13*(11), 1878. https://doi.org/10.3390/land13111878

Turner, B. L., Skole, D., Sanderson, S., Fischer, G., Fresco, L., & Leemans, R. (1995). *Land-use and land-cover change: Science/research plan* (IGBP Report No. 35). International Geosphere-Biosphere Programme.

United Nations, Department of Economic and Social Affairs, Population Division. (2018). *World urbanization prospects: The 2018 revision*. United Nations.

Winkler, K., Fuchs, R., Rounsevell, M., & Herold, M. (2021). Global land use changes are four times greater than previously estimated. *Nature Communications, 12*, 2501. https://doi.org/10.1038/s41467-021-22702-2

Yusuf, Y. Y. (2023). Spatio-temporal analysis of land use and land cover changes in Nguru Wetland, Yobe State, Nigeria. *International Journal of Environment, Ecology, Family and Urban Studies, 4*(2), 1–8.